

Artificial-reference tracking MPC with probabilistically validated performance on industrial embedded systems

Victor Gracia^{a,*}, Pablo Krupa^b, Filiberto Fele^a, Teodoro Alamo^a

^aDepartment of Systems Engineering and Automation, University of Seville, Seville, Spain

^bIMT School for Advanced Studies, Lucca, Italy

Abstract

Industrial embedded systems are typically used to execute simple control algorithms due to their low computational resources. Despite these limitations, the implementation of advanced control techniques such as Model Predictive Control (MPC) has been explored by the control community in recent years, typically considering simple linear formulations or explicit ones to facilitate the online computation of the control input. These simplifications often lack features and properties that are desirable in real-world environments. In this article, we present an efficient implementation for embedded systems of *MPC for tracking with artificial reference*, solved via a recently developed structure-exploiting first-order method. This formulation is tailored to a wide range of applications by incorporating essential practical features at a small computational cost, including integration with an offset-free scheme, back-off parameters that enable constraint tightening, and soft constraints that preserve feasibility under disturbances or plant-model mismatch. We accompany this with a framework for probabilistic performance validation of the closed-loop system over long-term operation. We illustrate the applicability of the approach on a Programmable Logic Controller (PLC), incorporated in a hardware-in-the-loop setup to control a nonlinear continuous stirred-tank reactor. The behavior of the closed-loop system is probabilistically validated with respect to constraint violations and the number of iterations required at each time step by the MPC optimization algorithm.

Keywords: Model predictive control, soft constraints, ADMM, industrial embedded system, probabilistic validation.

1. Introduction

In the process industry, control devices typically prioritize reliability and robustness over computational and memory resources. An example of a widely used industrial embedded system is Programmable Logic Controllers (PLC), which, due to their hardware limitations, have mostly been used to implement simple control laws, such as PID controllers or ladder logic (Alphonsus and Abdul-lah, 2016).

Compared to these control strategies, advanced control techniques offer advantages that can be interesting in industrial scenarios. In particular, Model Predictive Control (MPC) has received much attention due to its ability to optimize plant operation while satisfying system constraints, such as actuator limits and safety requirements (Camacho and Alba, 2007). In MPC, the control input is obtained at each sample time by solving an optimization problem that, based on a prediction model of the system, determines a system trajectory satisfying some optimality criterion. MPC has strong theoretical benefits, see Rawlings

et al. (2017), and has shown very good results on real systems, e.g., Abuin et al. (2022); Nubert et al. (2020); Krupa et al. (2021a); Moscato et al. (2024). This performance comes at the expense of solving the MPC optimization problem at each time step. Recent developments in efficient optimization methods, some specifically tailored to MPC problems (Frison and Diehl, 2020; Lowenstein et al., 2024; Krupa et al., 2020), have resulted in solution times in the order of milliseconds when implemented on computers or microcontrollers.

Significant effort has been made towards the implementation of MPC in industrial systems, e.g., Valencia-Palomo and Rossiter (2011), where a suboptimal explicit MPC controller for PLCs is proposed; Jerez et al. (2014), where custom embedded hardware architectures are developed for MPC deployment; or Krupa et al. (2021b), where MPC is tailored to PLC implementations accounting for relevant practical details. A common feature in the literature is to consider simple MPC formulations with linear prediction model, quadratic objective function, and box constraints. This choice is motivated by the fact that the resulting optimization problem of the MPC formulation is a simple instance of a Quadratic Programming (QP) problem. QP problems have been widely studied and can be efficiently solved, see Stellato et al. (2020); O'Donoghue

*Corresponding author

Email addresses: vgracia@us.es (Victor Gracia), pablo.krupa@imtlucca.it (Pablo Krupa), ffele@us.es (Filiberto Fele), talamo@us.es (Teodoro Alamo)

(2021). Among the different optimization methods used to solve QP problems, first-order methods (Beck, 2017) stand out as a particularly simple-to-implement class of methods that only require first-order information of the objective function and can leverage the problem sparsity, allowing memory-efficient implementations in embedded systems (Ferreau et al., 2017).

While these simple standard MPC formulations provide a good starting point for the implementation of MPC on embedded systems, they present drawbacks that limit their viability in industrial environments. External disturbances or mismatch between the prediction model and the real plant dynamics can lead to issues such as loss of feasibility, constraint violations, and steady-state offset when tracking constant references. Another feature often overlooked in the literature is the handling of joint state-input constraints, which can be desirable in many applications.

As a contribution of this article, we present an efficient implementation of a non-standard linear MPC formulation tailored to industrial embedded systems, augmented with features to address the aforementioned issues. In particular, we propose an *MPC for tracking* (MPCT) formulation with artificial reference (Krupa et al., 2024; Limon et al., 2008). This formulation provides several benefits with respect to simpler linear MPC formulations, such as an enlarged domain of attraction, or the ability to handle non-reachable references. Furthermore, the formulation considers joint state-input constraints and soft constraints (Kerrigan and Maciejowski, 2000), the latter ensuring recursive feasibility of the optimization problem. The MPC controller also incorporates back-off parameters (Santos et al., 2019) for constraint tightening to improve constraint satisfaction of the closed-loop system. For our efficient implementation, we build upon the recently developed first-order MPC solver proposed in Gracia et al. (2024a) and Gracia et al. (2024b), which was shown to provide low memory footprints and fast computation times. To allow piecewise-constant reference tracking without offset, we adopt the approach described in Maeder et al. (2009), including a state-disturbance estimator that adjusts the MPC reference to compensate for plant-model mismatch and constant additive disturbances.

Although this formulation is suitable for a wide range of real applications, many of its features involve parameters that need careful adjustment to achieve adequate performance in real scenarios, where operating conditions are often not ideal. Consequently, parameter selection plays a critical role in ensuring the suitable and safe operation of the plant under real conditions. To address this challenge, we propose a framework that facilitates the configuration of the controller while providing probabilistic guarantees of performance. In particular, we extend the probabilistic performance validation method in Karg et al. (2021) to allow the validation of several aspects of the control setup. Furthermore, we demonstrate how it can be applied for the validation of the long-term closed-loop system operation.

To illustrate the benefits of the proposed MPC scheme

and the probabilistic validation approach, we implement the controller on a Siemens S7-1500 PLC in a Hardware-in-the-Loop (HiL) setup to control a Continuous Stirred-Tank Reactor (CSTR), showing that advanced, practical MPC formulations can be deployed in industrial embedded systems with solution times in the order of a few seconds. The solver is coded using standard IEC 61131-3 programming languages and adapted to PLC requirements, see Krupa et al. (2021b, §V). We probabilistically certify that the closed-loop system does not violate the constraints beyond a given threshold, while also providing a probabilistic upper bound on the maximum number of iterations of the optimization solver. The latter ensures suitable computational times to obtain the control input, an essential factor in real-time control applications.

The remainder of this article is structured as follows. Section 2 presents the problem setting and the nominal MPCT formulation. Section 3 details how the formulation is augmented for its real-world implementation, including the offset-free scheme, back-off parameters, and soft constraints. Section 4 illustrates the formal framework for the probabilistic validation of the control setup. Section 5 explains the structure-exploiting MPCT solver, suitable for embedded systems implementations. Section 6 presents the experimental results. Section 7 closes the article.

Notation: The identity matrix of size n is denoted as \mathbf{I}_n . A p -dimensional column vector with all its elements equal to 1 is denoted as $\mathbf{1}_p$. The j -th element of a vector $v \in \mathbb{R}^n$ is written as $v_{(j)}$. The set of integers is denoted as \mathbb{I} , with $\mathbb{I}_i^j = \{i, i+1, \dots, j\}$ for integers $i < j$. Given a positive definite matrix M , we define $\|v\|_M \doteq \sqrt{v^\top M v}$. The function $\max(\cdot)$ returns the maximum among the scalars received as input. Given a vector $v \in \mathbb{R}^n$, $\text{diag}(v)$ is a diagonal matrix with diagonal v . The block-diagonal matrix formed by placing the matrices M_1, \dots, M_N along its diagonal is denoted by $\text{blkdiag}(M_1, \dots, M_N)$. The column vector formed by the concatenation of column vectors v_1, \dots, v_n , possibly of different dimensions, is expressed as (v_1, \dots, v_n) . Symbols \leq ($<$) and \geq ($>$) denote component-wise inequalities when applied to vectors. The indicator function on a set $\mathcal{C} \subseteq \mathbb{R}^n$ is denoted by $\delta_{\mathcal{C}}: \mathcal{C} \rightarrow \{0, +\infty\}$, i.e., $\delta_{\mathcal{C}}(x) = 0$ if $x \in \mathcal{C}$ and $\delta_{\mathcal{C}}(x) = +\infty$ if $x \notin \mathcal{C}$. Given a random vector $w \sim \mathcal{W}$, the notation $P_{\mathcal{W}}\{\cdot\}$ denotes the probability of an event involving w .

2. Problem statement and MPC formulation

In this article, we consider the problem of controlling a possibly nonlinear time-invariant system, modeled by the discrete-time equations

$$x(k+1) = f_p(x(k), u(k), d(k)), \quad (1a)$$

$$y(k) = g_p(x(k), d(k)), \quad (1b)$$

where $x(k) \in \mathbb{R}^n$, $u(k) \in \mathbb{R}^m$, $y(k) \in \mathbb{R}^p$ and $d(k) \in \mathbb{R}^{n_d}$ are the state, input, measured output and disturbance of

the plant at sample time k , respectively. In our subsequent developments, f_p and g_p are only required to be continuous at all equilibrium points. Moreover, without loss of generality, we assume that $g_p(0, 0) = 0$, and that the origin is an equilibrium point, i.e., $f_p(0, 0, 0) = 0$.

The control objective is to make $y(k)$ track a piecewise constant reference $y_r(k) \in \mathbb{R}^p$ while satisfying the system constraints

$$(x(k), u(k)) \in \mathcal{Z}, \forall k \geq 0, \quad (2)$$

where $\mathcal{Z} \subseteq \mathbb{R}^{n+m}$ is a non-empty, closed and convex set that contains the origin in its interior.

This objective can be achieved by using a tracking MPC controller (Rawlings et al., 2017). As we consider the case where the controller is implemented on a limited hardware platform, solver efficiency is essential. While simple linear MPC formulations can be compatible with such requirement, their practical performance is limited by factors such as modeling errors or unknown disturbances. A contribution of this work is to provide an advanced, efficiently solvable formulation suitable for real control scenarios, achieved by incorporating key practical features.

We begin by considering the linear state-space prediction model

$$x_{i+1} = Ax_i + Bu_i, \quad (3a)$$

$$y_i = Cx_i, \quad (3b)$$

where $x_i \in \mathbb{R}^n$, $u_i \in \mathbb{R}^m$ and $y_i \in \mathbb{R}^p$ are the state, input, and output vectors of the model at prediction step i , respectively. This model captures the dynamics of (1) in a neighbourhood of the origin, and is assumed to be controllable and observable. Models of the form of (3) can be obtained using standard procedures, e.g., through system identification using experimental data, or by linearization of a high-fidelity nonlinear model of the real system.

The dynamics (3) are subject to the linear constraints

$$\underline{x} \leq x_i \leq \bar{x}, \quad (4a)$$

$$\underline{u} \leq u_i \leq \bar{u}, \quad (4b)$$

$$\underline{h} \leq Ex_i + Fu_i \leq \bar{h}, \quad (4c)$$

where $\underline{x}, \bar{x} \in \mathbb{R}^n$, $\underline{u}, \bar{u} \in \mathbb{R}^m$ and $\underline{h}, \bar{h} \in \mathbb{R}^{n_p}$ satisfy, respectively, $\underline{x} < \bar{x}$, $\underline{u} < \bar{u}$ and $\underline{h} < \bar{h}$. Equations (4) characterize a non-empty convex set resulting from a linearization or approximation of the real system constraints (2).

Our work is based on the *MPC for Tracking* (MPCT) with artificial reference formulation (Limon et al., 2008). MPCT is a class of MPC formulations characterized by the addition of an artificial reference as part of the decision variables of its optimization problem. In the nominal case, i.e., when (3) matches (1) and there are no disturbances in (1), this feature provides several benefits with respect to traditional MPC formulations, at the expense of some additional complexity in its underlying optimization problem. These benefits include: increased domain of attraction, recursive feasibility even if the reference is

changed online, and asymptotic stability to the admissible steady state that is “closest” to the given reference.

The MPCT control law is derived from the solution of the optimization problem

$$\min_{\substack{\mathbf{x}, \mathbf{u}, \\ x_s, u_s}} V_o(x_s, u_s) + \sum_{i=0}^{N-1} \ell(x_i, u_i) \quad (5a)$$

$$\text{s.t. } x_0 = \hat{x}(k), \quad (5b)$$

$$(3a), \quad i \in \mathbb{I}_0^{N-2}, \quad (5c)$$

$$x_s = Ax_{N-1} + Bu_{N-1}, \quad (5d)$$

$$x_s = Ax_s + Bu_s, \quad (5e)$$

$$(4a), \quad i \in \mathbb{I}_1^{N-1}, \quad (5f)$$

$$(4b), \quad i \in \mathbb{I}_0^{N-1}, \quad (5g)$$

$$(4c), \quad i \in \mathbb{I}_0^{N-1}, \quad (5h)$$

$$\underline{x} \leq x_s \leq \bar{x}, \quad \underline{u} \leq u_s \leq \bar{u}, \quad (5i)$$

$$\underline{h} \leq Ex_s + Fu_s \leq \bar{h}, \quad (5j)$$

where the stage cost function $\ell(\cdot)$ is defined as

$$\ell(x, u) \doteq \|x - x_s\|_Q^2 + \|u - u_s\|_R^2,$$

the offset cost function $V_o(\cdot)$ is given by

$$V_o(x_s, u_s) \doteq \|x_s - x_r(k)\|_T^2 + \|u_s - u_r(k)\|_S^2,$$

the weight matrices $Q \in \mathbb{R}^{n \times n}$, $R \in \mathbb{R}^{m \times m}$, $T \in \mathbb{R}^{n \times n}$ and $S \in \mathbb{R}^{m \times m}$ are positive definite, and $\hat{x}(k)$ is an estimate of the current state of the system. The decision variables are the predicted states and inputs $\mathbf{x} = (x_0, \dots, x_{N-1})$, $\mathbf{u} = (u_0, \dots, u_{N-1})$, along the prediction horizon of length $N > 0$, together with the artificial reference $(x_s, u_s) \in \mathbb{R}^{n+m}$, forced to be an admissible steady state of (3) satisfying (4) by means of the constraints (5e), (5i) and (5j)¹. Note that the terminal predicted state x_N is forced to be equal to x_s via the terminal constraint (5d).

The MPCT formulation (5) allows to deal with references (x_r, u_r) that are not admissible, i.e., that do not satisfy the model constraints (4), and/or that are not steady states of (3). Under nominal conditions, if a constant reference (x_r, u_r) is admissible, the closed-loop system will asymptotically converge to it; otherwise, it will asymptotically converge to the admissible steady state (x°, u°) that minimizes $\|x^\circ - x_r\|_T^2 + \|u^\circ - u_r\|_S^2$, i.e., to the closest admissible steady state, as measured by the matrices T and S . For an in-depth review of the literature on MPCT, we refer the reader to the tutorial article Krupa et al. (2024).

Remark 1. While the tracking objective is stated in terms of the output of (1), the formulation (5) requires the state-input reference pair $(x_r(k), u_r(k))$. This is clarified in Section 3.1, where we include an offset-free strategy allowing to obtain $(x_r(k), u_r(k))$ from the output reference $y_r(k)$.

¹In the nominal case, the artificial reference constraints (5i) and (5j) require an arbitrarily small tightening for guaranteed stability (Limon et al., 2008). We omit this detail in formulation (5), as the inclusion of soft constraints in Section 3.3 removes this requirement.

3. Practical MPCT formulation

Despite the aforementioned benefits of the formulation (5) compared to simpler MPC formulations, its performance may still not be adequate in real-world applications, where the nominal conditions often do not hold. Model mismatch, discrepancies between the model constraints (4) and the actual system constraints (2), and external disturbances can lead to steady-state offset when tracking constant references, or even to infeasibility of the MPCT optimization problem, in which case the controller is unable to provide a control input for the system. The following section shows how the MPCT formulation (5) can be tailored to real-world control applications by including key practical features, compatibly with industrial embedded hardware capabilities.

To this end, we now discuss the inclusion of three elements in the MPCT formulation (5): an offset-free strategy to cancel the offset derived from plant-model mismatch and disturbances; back-off parameters that tighten the model constraints (4) to make the controlled system (1) satisfy the actual constraints (2); and the softening of most MPC inequality constraints, resulting in a formulation whose optimization problem is always feasible.

3.1. Disturbance rejection and offset-free MPC

We use the approach described in Maeder et al. (2009) to address disturbance rejection and offset cancelation. We focus on the case where the number of measured outputs p is equal to the number of disturbances considered in the model. As a result, the model (3) is augmented as

$$x_{i+1} = Ax_i + Bu_i + B_d d_i, \quad (6a)$$

$$d_{i+1} = d_i, \quad (6b)$$

$$y_i = Cx_i + d_i, \quad (6c)$$

where $B_d \in \mathbb{R}^{n \times p}$ and $d_i \in \mathbb{R}^p$. At each time step k , a Luenberger observer is used to update the estimates \hat{x} and \hat{d} of x and d as

$$\begin{bmatrix} \hat{x}(k+1) \\ \hat{d}(k+1) \end{bmatrix} = \begin{bmatrix} A & B_d \\ 0 & \mathbf{I}_p \end{bmatrix} \begin{bmatrix} \hat{x}(k) \\ \hat{d}(k) \end{bmatrix} + \begin{bmatrix} B \\ 0 \end{bmatrix} u(k) + \begin{bmatrix} L_x \\ L_d \end{bmatrix} (C\hat{x}(k) + \hat{d}(k) - y(k)), \quad (7)$$

where $L_x \in \mathbb{R}^{n \times p}$ and $L_d \in \mathbb{R}^{p \times p}$ are the observer gains, which must be designed so as to ensure the stability of the observer (Maeder et al., 2009).

At each sample time k , the reference $(x_r(k), u_r(k))$ provided to the MPCT is updated by solving the linear system

$$\begin{bmatrix} A - \mathbf{I}_n & B \\ C & 0 \end{bmatrix} \begin{bmatrix} x_r(k) \\ u_r(k) \end{bmatrix} = \begin{bmatrix} -B_d \hat{d}(k) \\ y_r(k) - \hat{d}(k) \end{bmatrix}. \quad (8)$$

Provided that system (8) is solvable, the solution may not be unique or may not satisfy the system constraints (4). Since the MPCT can handle nonadmissible reference pairs $(x_r(k), u_r(k))$, any solution of system (8) can directly serve as a reference.

3.2. Tightening of constraints

The use of the formulation (5) to control the system (1) does not guarantee the satisfaction of the constraints (2). This is due to: the possible discrepancy between the constraints of the MPC model (4) and those of the real system (2), the inability of the controller to predict the actual evolution of the plant given the mismatch between the real system (1) and the model (3), and the presence of external disturbances.

To address this issue, we take the approach of tightening the model constraints (4) by means of back-off parameters (Santos et al., 2019), to ensure that the plant (1) actually satisfies its true constraints (2) during operation. In particular, the state and coupled state-input constraints of (5) can be tightened by introducing nonnegative back-off parameters $\underline{\eta}_x, \bar{\eta}_x \in \mathbb{R}^n$, $\underline{\eta}_h, \bar{\eta}_h \in \mathbb{R}^{n_h}$. The resulting set of tightened model constraints is

$$\underline{x} + \underline{\eta}_x \leq x_i \leq \bar{x} - \bar{\eta}_x, \quad i \in \mathbb{I}_1^{N-1}, \quad (9a)$$

$$\underline{x} + \underline{\eta}_x \leq x_s \leq \bar{x} - \bar{\eta}_x, \quad (9b)$$

$$\underline{h} + \underline{\eta}_h \leq Ex_i + Fu_i \leq \bar{h} - \bar{\eta}_h, \quad i \in \mathbb{I}_0^{N-1}, \quad (9c)$$

$$\underline{h} + \underline{\eta}_h \leq Ex_s + Fu_s \leq \bar{h} - \bar{\eta}_h, \quad (9d)$$

where $\underline{x} + \underline{\eta}_x < \bar{x} - \bar{\eta}_x$ and $\underline{h} + \underline{\eta}_h < \bar{h} - \bar{\eta}_h$. Although possible, input constraint tightening is not considered, as they typically represent real actuator limits.

In Section 4, we present a formal validation approach that will enable us to select the values of the back-off parameters in (9), providing probabilistic bounds on the satisfaction of the constraints (2) during online operation.

3.3. Soft constraints

One of the well-known limitations of MPC when considering hard constraints, such as in (5), is the possible infeasibility of the optimization problem for a given $\hat{x}(k)$. In this situation, the MPC controller cannot provide a control input, requiring the use of an auxiliary controller. This situation is expected when using linear MPC to control a nonlinear system, either due to disturbances or to plant-model mismatch. To deal with this issue, we relax hard inequality constraints into *soft constraints* (Kerrigan and Maciejowski, 2000; Wabersich et al., 2022), whose violation is penalized in the cost function. This ensures that the optimization problem is always feasible, enabling the controller to always compute a control input.

In this article, we take the encoding of soft constraints presented in Gracia et al. (2024b). As an example, the constraint (4a) can be softened by replacing it with a non-smooth term as

$$\gamma_\beta(x_i; \bar{x}, \underline{x}) \doteq \sum_{j=1}^n \beta_{(j)} \max(x_{i(j)} - \bar{x}_{(j)}, \underline{x}_{(j)} - x_{i(j)}, 0) \quad (10)$$

in the objective function, where $\beta \in \mathbb{R}^n$ is a positive vector of coefficients penalizing the constraint violation of each

element of x_i . The remaining inequality constraints of the formulation (5) can be relaxed in the same manner. This encoding retains the simple structure of the MPCT optimization problem, which is exploited by the numerical solver, as detailed in Section 5.

3.4. Practical MPCT formulation

Here we summarize the formulation to be implemented on the embedded system, which includes the features mentioned in the previous subsections. Defining the notation $h_i \doteq Ex_i + Fu_i$, $i \in \mathbb{I}_0^{N-1}$, $h_s \doteq Ex_s + Fu_s$, and the vector $\vartheta \doteq (h_0, x_1, u_1, h_1, \dots, x_{N-1}, u_{N-1}, h_{N-1}, x_s, u_s, h_s) \in \mathbb{R}^{n_\vartheta}$, where $n_\vartheta = n_h + N(n + m + n_h)$, the MPCT formulation (5) can be cast in its practical variant as

$$\min_{\mathbf{x}, \mathbf{u}, u_s} V_o(x_s, u_s) + \gamma_\beta(\vartheta; \bar{\vartheta}, \underline{\vartheta}) + \sum_{i=0}^{N-1} \ell(x_i, u_i) \quad (11a)$$

$$\text{s.t. } x_0 = \hat{x}(k), \quad (11b)$$

$$x_{i+1} = Ax_i + Bu_i + B_d\hat{d}(k), \quad i \in \mathbb{I}_0^{N-2}, \quad (11c)$$

$$x_s = Ax_{N-1} + Bu_{N-1} + B_d\hat{d}(k), \quad (11d)$$

$$x_s = Ax_s + Bu_s + B_d\hat{d}(k), \quad (11e)$$

$$\underline{u} \leq u_0 \leq \bar{u}, \quad (11f)$$

where the term used to include soft constraints $\gamma_\beta(\cdot)$ penalizes the violation of constraints for the variables included in ϑ . Note that ϑ collects all the decision variables except for x_0 , as it does not present box constraints, and u_0 , which keeps its hard constraint (11f) to provide a control action satisfying the physical limits of the actuators. Additionally, ϑ includes the variables h_i , $i \in \mathbb{I}_0^{N-1}$, and h_s , which are used to soften the coupled state-input constraints defined in (5h) and (5j). The vectors $\underline{\vartheta}, \bar{\vartheta} \in \mathbb{R}^{n_\vartheta}$ collect the bounds of the box constraints in ϑ , considering also the tightening introduced by the back-off parameters, i.e.,

$$\begin{aligned} \underline{\vartheta} &\doteq (h + \underline{\eta}_h, x + \underline{\eta}_x, \underline{u}, h + \underline{\eta}_h, \dots, x + \underline{\eta}_x, \underline{u}, h + \underline{\eta}_h), \\ \bar{\vartheta} &\doteq (\bar{h} - \bar{\eta}_h, \bar{x} - \bar{\eta}_x, \bar{u}, \bar{h} - \bar{\eta}_h, \dots, \bar{x} - \bar{\eta}_x, \bar{u}, \bar{h} - \bar{\eta}_h). \end{aligned}$$

The use of soft constraints in (11) leads to an optimization problem that is always feasible if the length of the prediction horizon N is greater than the controllability index of the augmented system (6), see Gracia et al. (2024b). Moreover, there exists a sufficiently large β such that the optimal solution of the soft-constrained formulation (11) coincides with the optimal solution of its equivalent hard-constrained version whenever the latter is feasible; this is due to the exact penalty property of $\gamma_\beta(\cdot)$ (Fletcher, 2000, Thm. 14.3.1), (Kerrigan and Maciejowski, 2000).

4. Probabilistic validation of the controller

In the previous section, we have described an advanced MPC formulation with features that enable its applicability in real control scenarios. However, selecting the con-

troller parameters so that the real plant operates as desired is not trivial. A practical approach is to define several controllers based on different parameter values, test their behavior on a number of experiments, and select the most satisfactory one. Still, choosing a configuration is challenging in many cases, as the selected controller may be unsuitable in scenarios other than those considered in the experiments, or it may not provide a good balance in every aspect of interest, e.g., control response, constraint satisfaction or computation time. Therefore, a methodology to suitably compare the controllers in a wide range of scenarios and validate their long-term operation is desirable, preferably enabling the selection of a controller that provides solid performance according to several criteria.

For this, we propose a performance validation approach to select a controller that satisfies, in a probabilistic sense, multiple performance requirements (Mammarella et al., 2020). In particular, we extend the main result in Karg et al. (2021) to enable the selection of one among $M \geq 1$ candidate controllers with probabilistic guarantees across $K \geq 1$ performance metrics.

Let $w \in \mathbb{R}^{n_w}$ be a vector collecting the uncertain variables that uniquely determine² a trajectory of the system when in closed-loop with a controller κ (e.g., system disturbances, communication delays, etc.). We note that the size of w is typically proportional to the duration of the trajectory, which we consider of N_t time steps. We assume that w is a random vector that follows some (unknown) probability distribution \mathcal{W} . Let $\phi(w; \kappa, N_t) : \mathbb{R}^{n_w} \rightarrow \mathbb{R}$ be a closed-loop performance indicator (Karg et al., 2021, Definition 1) that returns a scalar evaluating the performance of the controller κ under the realization $w \sim \mathcal{W}$. We define $\phi(\cdot)$ such that lower values indicate better performance. In Section 6, we define performance indicators to assess the satisfaction of the constraints (2) and the maximum number of iterations of the optimization solver, for which probabilistic bounds will be established.

Given N_s independent and identically distributed (i.i.d.) samples $w_j \sim \mathcal{W}$, $j \in \mathbb{I}_1^{N_s}$, M controllers κ_i , $i \in \mathbb{I}_1^M$, and K performance indicators $\phi^\ell(\cdot)$, $\ell \in \mathbb{I}_1^K$, let us denote $\phi_i^\ell(w_j) \doteq \phi^\ell(w_j; \kappa_i, N_t)$ as the performance of the controller κ_i under the uncertainty realization w_j , as evaluated by the indicator ϕ^ℓ . We define $\phi_i^{\ell, [r]}$ as the r -th worst performance among the N_s samples, i.e., the r -th largest value of the set $\{\phi_i^\ell(w_1), \dots, \phi_i^\ell(w_{N_s})\}$.

We are now ready to present the formal validation procedure, applicable to any set of controller parameters.

Proposition 1. *Given the controllers κ_i , $i \in \mathbb{I}_1^M$, and the performance indicators $\phi^\ell(\cdot)$, $\ell \in \mathbb{I}_1^K$, suppose that N_s i.i.d. scenarios $w_j \sim \mathcal{W}$, $j \in \mathbb{I}_1^{N_s}$, are generated. Then, for any choice of the integer $1 \leq r \leq N_s$, it holds with probability no smaller than $1 - \delta$ that*

$$P_{\mathcal{W}}\{\phi_i^\ell(w) > \phi_i^{\ell, [r]}\} \leq \epsilon, \quad i \in \mathbb{I}_1^M, \quad \ell \in \mathbb{I}_1^K, \quad (12)$$

²“Uniquely determine” refers to the fact that a given realization w always results in the same system trajectory.

provided that

$$\sum_{q=0}^{r-1} \binom{N_s}{q} \epsilon^q (1-\epsilon)^{N_s-q} \leq \frac{\delta}{MK}. \quad (13)$$

Proof. Proposition 1 follows directly from Theorem 1 in Karg et al. (2021). It suffices to observe that considering $K \geq 2$ performance indicators implies accounting for a greater number of statistical events with respect to the original theorem. \square

We note that (13) is satisfied if

$$N_s \geq \frac{1}{\epsilon} \left(r - 1 + \ln \frac{MK}{\delta} + \sqrt{2(r-1)\ln \frac{MK}{\delta}} \right). \quad (14)$$

Condition (14) can be used to determine a sufficient number N_s of closed-loop experiments to ensure that (12) holds with a probability of at least $1 - \delta$. In turn, equation (12) states that, when selecting a specific controller κ_i , $i \in \mathbb{I}_1^M$, and a performance indicator ϕ_i^ℓ , $\ell \in \mathbb{I}_1^K$, if we take a new realization $w \sim \mathcal{W}$,

$$\phi_i^\ell(w) \leq \phi_i^{\ell,[r]}$$

holds with probability larger than $1 - \epsilon$. That is, in a new experiment using the controller κ_i , the probability of obtaining a performance (as measured by ϕ^ℓ) worse or equal to the r -th worst among the N_s validation experiments is at most ϵ , with confidence at least $1 - \delta$. Note that the parameter r is selected so as to adjust the conservativeness of the probabilistic bounds, at the expense of requiring a larger number of experiments (as visible from (14)).

Remark 2. Considering multiple performance indicators ($K \geq 2$) leads to a greater number of closed-loop experiments. Nonetheless, K always appears inside logarithmic terms in (14), meaning that N_s does not grow significantly in practice.

Remark 3. When one of the M controllers is selected after applying Proposition 1 for $K \geq 2$, the probability that a new $w \sim \mathcal{W}$ results in a better performance than the r -th worst case out of the N_s experiments is guaranteed (with confidence at least $1 - \delta$) to be at least $1 - \epsilon$ for each performance indicator individually. However, no guarantee is provided that, for a given $w \sim \mathcal{W}$, all K performance indicators will simultaneously be better than their respective r -th worst cases. Nevertheless, when ϵ is small, simultaneous satisfaction is often observed empirically.

5. Implementation of the MPC solver

This section presents the practical algorithmic implementation of the MPCT formulation (11). To this end, we combine the solver of Gracia et al. (2024a) based on the Alternating Direction Method of Multipliers (ADMM) algorithm (Boyd et al., 2011) tailored to exploit the MPCT

Algorithm 1: ADMM

```

Require:  $v^0, \lambda^0, \rho > 0, \epsilon_p > 0, \epsilon_d > 0$ 
1  $l \leftarrow 0$ 
2 repeat
3    $z^{l+1} \leftarrow \arg \min_z \mathcal{L}_\rho(z, v^l, \lambda^l)$ 
4    $v^{l+1} \leftarrow \arg \min_v \mathcal{L}_\rho(z^{l+1}, v, \lambda^l)$ 
5    $\lambda^{l+1} \leftarrow \lambda^l + \rho(Dz^{l+1} - v^{l+1})$ 
6    $l \leftarrow l + 1$ 
7 until  $\|Dz^l - v^l\|_\infty \leq \epsilon_p$  and  $\|v^l - v^{l-1}\|_\infty \leq \epsilon_d$ 
Output:  $\tilde{z}^* \leftarrow z^l, \tilde{v}^* \leftarrow v^l, \tilde{\lambda}^* \leftarrow \lambda^l$ 

```

problem structure, with the approach presented in Gracia et al. (2024b) to implement the soft constraints. We emphasize that by exploiting the MPCT problem structure, we achieve significant reductions in memory requirement and computation time per iteration compared to general-purpose QP solvers such as Stellato et al. (2020); O'Donoghue (2021), even when these leverage sparse matrix representations and sparse linear algebra subroutines.

Since the experimental results in Section 6 are of primary interest, we briefly review how the ADMM algorithm is used to solve (11), and how the soft constraints are handled without affecting the problem structure, thus preserving efficiency. For a detailed explanation of the solver, see Gracia et al. (2024a,b). An implementation of this solver in C programming language can be found in the open-source Matlab package SPCIES (Krupa et al., 2020).

Consider the optimization problem

$$\min_{z,v} f(z) + g(v) \quad (15a)$$

$$\text{s.t. } Dz = v, \quad (15b)$$

where $z \in \mathbb{R}^{n_z}$ and $v \in \mathbb{R}^{n_v}$ are the optimization variables, $D \in \mathbb{R}^{n_v \times n_z}$, and $f : \mathbb{R}^{n_z} \rightarrow \mathbb{R} \cup \{+\infty\}$, $g : \mathbb{R}^{n_v} \rightarrow \mathbb{R} \cup \{+\infty\}$ are convex, closed, proper functions. For problem (15), ADMM considers an augmented Lagrangian $\mathcal{L}_\rho : \mathbb{R}^{n_z} \times \mathbb{R}^{n_v} \times \mathbb{R}^{n_v} \rightarrow \mathbb{R} \cup \{+\infty\}$ given by

$$\mathcal{L}_\rho(z, v, \lambda) = f(z) + g(v) + \lambda^\top (Dz - v) + \frac{\rho}{2} \|Dz - v\|_2^2, \quad (16)$$

where $\lambda \in \mathbb{R}^{n_v}$ is the vector of dual variables and $\rho > 0$ is a regularization parameter. The steps of ADMM are given by Algorithm 1, which, at each iteration l , first minimizes (16) with respect to z , then with respect to v , and finally updates the dual variables λ . Starting from any $(z^0, v^0, \lambda^0) \in \mathbb{R}^{n_z} \times \mathbb{R}^{n_v} \times \mathbb{R}^{n_v}$, the iterates (z^l, v^l, λ^l) of Algorithm 1 asymptotically converge to an optimal solution (z^*, v^*, λ^*) of (15), assuming that one exists (He and Yuan, 2012). In practice, however, the algorithm is terminated when the exit conditions in Step 7 are satisfied, where $\epsilon_p > 0$ and $\epsilon_d > 0$ are exit tolerances.

To pose the MPCT problem (11) in the form of (15), we take

$$z \doteq (x_0, u_0, \dots, x_{N-1}, u_{N-1}, x_s, u_s) \in \mathbb{R}^{n_z},$$

collecting the decision variables of (11), with $n_z = (N + 1)(n + m)$;

$$v \doteq (\tilde{x}_0, \tilde{u}_0, \tilde{h}_0, \dots, \tilde{x}_{N-1}, \tilde{u}_{N-1}, \tilde{h}_{N-1}, \tilde{x}_s, \tilde{u}_s, \tilde{h}_s) \in \mathbb{R}^{n_v},$$

with $n_v = (N + 1)(n + m + n_h)$, which contains copies of the variables in z to decouple the equality and inequality constraints of (11), and includes variables \tilde{h} to handle the joint state-input constraints;

$$D = \text{blkdiag} \left(\begin{bmatrix} \mathbf{I}_n & 0 \\ 0 & \mathbf{I}_m \\ E & F \end{bmatrix}, \dots, \begin{bmatrix} \mathbf{I}_n & 0 \\ 0 & \mathbf{I}_m \\ E & F \end{bmatrix} \right),$$

which relates vectors z and v through the constraint (15b);

$$f(z) = \frac{1}{2} z^\top H z + q^\top z + \delta_{\{z: Gz=b\}}(z),$$

where, defining $m_z = (N + 1)n$,

$$H = \begin{bmatrix} Q & 0 & \cdots & -Q & 0 \\ 0 & R & \cdots & 0 & -R \\ 0 & 0 & \ddots & \vdots & \vdots \\ -Q & 0 & \cdots & NQ + T & 0 \\ 0 & -R & \cdots & 0 & NR + S \end{bmatrix} \in \mathbb{R}^{n_z \times n_z}, \quad (17a)$$

$$q = -(0, \dots, 0, T x_r(k), S u_r(k)) \in \mathbb{R}^{n_z}, \quad (17b)$$

$$G = \begin{bmatrix} \mathbf{I}_n & 0 & 0 & 0 & \cdots & 0 \\ A & B & -\mathbf{I}_n & 0 & \cdots & 0 \\ 0 & \ddots & \ddots & \ddots & 0 & \vdots \\ 0 & 0 & A & B & -\mathbf{I}_n & 0 \\ 0 & 0 & 0 & 0 & (A - \mathbf{I}_n) & B \end{bmatrix} \in \mathbb{R}^{m_z \times n_z}, \quad (17c)$$

$$b = (\hat{x}(k), -B_d \hat{d}(k), \dots, -B_d \hat{d}(k)) \in \mathbb{R}^{m_z}, \quad (17d)$$

and, defining $\tilde{\vartheta}$ as a trimmed version of v without $(\tilde{x}_0, \tilde{u}_0)$, i.e., $\tilde{\vartheta} \doteq (\tilde{h}_0, \tilde{x}_1, \tilde{u}_1, \tilde{h}_1, \dots, \tilde{x}_{N-1}, \tilde{u}_{N-1}, \tilde{h}_{N-1}, \tilde{x}_s, \tilde{u}_s, \tilde{h}_s)$,

$$g(v) = \delta_{\{\tilde{u}_0: \underline{u} \leq \tilde{u}_0 \leq \bar{u}\}}(\tilde{u}_0) + \gamma_{\beta/2}(\tilde{\vartheta}; \bar{\vartheta}, \underline{\vartheta}).$$

Step 3 in Algorithm 1 solves the equality-constrained QP problem

$$z^{l+1} = \arg \min_z \frac{1}{2} z^\top P z + (p^l)^\top z \quad (18a)$$

$$\text{s.t. } Gz = b, \quad (18b)$$

where $P = H + \rho D^\top D$ and $p^l = q + D^\top(\lambda^l - \rho v^l)$. Given that D has full column rank³, the Hessian P in (18a) is positive definite. Moreover, since the system (3) is assumed to be controllable, G has full row rank. Consequently, the solution of problem (18) is unique.

Solving (18) is the most computationally demanding step of Algorithm 1. To attain efficiency, we exploit the

³The vector v includes \tilde{x}_0 to ensure that D has full column rank.

particular semi-banded structure⁴ of P . Our method works as follows. First, we note that the equality-constrained problem (18) can be solved using the explicit solution method described in Boyd (2009, §5.5.3). This method relies on finding a solution of the Karush-Kuhn-Tucker (KKT) optimality conditions, which in this case amounts to solving a linear system of equations. This, in turn, can be decomposed in three simpler linear systems

$$P\xi = p^l, \quad (19a)$$

$$W\mu^* = -(G\xi + b), \quad (19b)$$

$$Pz^{l+1} = -(G^\top \mu^* + p^l), \quad (19c)$$

where $W \doteq GP^{-1}G^\top \in \mathbb{R}^{m_z \times m_z}$ is also semi-banded, and $\mu^* \in \mathbb{R}^{m_z}$ is the dual optimal solution of problem (18). We leverage the Woodbury matrix identity (Tylavsky and Sohie, 1986) to decompose the semi-banded matrices arising in (19). In particular, steps (19a) and (19c) are computationally inexpensive, as each of them involves solving two block-diagonal systems separated by a simpler step involving two small-scaled matrix-vector products. In turn, (19b) is more demanding due to the structure of W , as instead of the two block-diagonal systems, it requires solving two systems of the form $\tilde{\Gamma}w = c$, where $\tilde{\Gamma}$ has a specific banded-diagonal structure. This structure is exploited in Krupa et al. (2021b), where the authors use the Cholesky factorization of $\tilde{\Gamma}$ and apply forward-backward substitution; a strategy we also adopt in our solver.

Step 4 of Algorithm 1 implies solving the separable optimization problem

$$\begin{aligned} v^{l+1} = \arg \min_v \frac{\rho}{2} \|Dz^{l+1} - v\|_2^2 - (\lambda^l)^\top v + \gamma_{\beta/2}(\tilde{\vartheta}; \bar{\vartheta}, \underline{\vartheta}) \\ \text{s.t. } \underline{u} \leq \tilde{u}_0 \leq \bar{u}. \end{aligned}$$

Defining $c_{(j)} \doteq (Dz^{l+1})_{(j)} + \frac{1}{\rho} \lambda_{(j)}^l$, it follows from the definition of D that the components of v^{l+1} related to \tilde{x}_0 , i.e., $v_{(j)}^{l+1}$, $j \in \mathbb{I}_1^n$, can be computed explicitly as

$$v_{(j)}^{l+1} = c_{(j)} = z_{(j)}^{l+1} + \frac{1}{\rho} \lambda_{(j)}^l,$$

and the components related to \tilde{u}_0 , i.e., $v_{(j)}^{l+1}$, $j \in \mathbb{I}_{n+1}^{n+m}$, as

$$\begin{aligned} v_{(j)}^{l+1} &= \min \left(\max \left(c_{(j)}, \underline{u}_{(j-n)} \right), \bar{u}_{(j-n)} \right) \\ &= \min \left(\max \left(z_{(j)}^{l+1} + \frac{1}{\rho} \lambda_{(j)}^l, \underline{u}_{(j-n)} \right), \bar{u}_{(j-n)} \right). \end{aligned}$$

The remaining elements of v^{l+1} , i.e., $v_{(j)}^{l+1}$, $j \in \mathbb{I}_{n+m+1}^{n_v}$, can be computed explicitly as follows. Defining $i \doteq j - n - m$,

$$v_{(j)}^{l+1} = \begin{cases} c_{(j)} + \frac{\beta_{(i)}}{2\rho} & \text{if } c_{(j)} + \frac{\beta_{(i)}}{2\rho} \leq \underline{\vartheta}_{(i)}, \\ \underline{\vartheta}_{(i)} & \text{if } c_{(j)} + \frac{\beta_{(i)}}{2\rho} > \underline{\vartheta}_{(i)} \text{ and } c_{(j)} < \underline{\vartheta}_{(i)}, \\ c_{(j)} & \text{if } \underline{\vartheta}_{(i)} \leq c_{(j)} \leq \bar{\vartheta}_{(i)}, \\ \bar{\vartheta}_{(i)} & \text{if } c_{(j)} > \bar{\vartheta}_{(i)} \text{ and } c_{(j)} - \frac{\beta_{(i)}}{2\rho} < \bar{\vartheta}_{(i)}, \\ c_{(j)} - \frac{\beta_{(i)}}{2\rho} & \text{if } c_{(j)} - \frac{\beta_{(i)}}{2\rho} \geq \bar{\vartheta}_{(i)}. \end{cases}$$

⁴See Gracia et al. (2024a, Definition 1).

This implementation of MPCT leads to solution times comparable to those of the standard MPC equivalent formulation, that is, without the artificial reference and soft constraints; see [Gracia et al. \(2024a,b\)](#) for further details.

To further improve the performance of the algorithm, we employ a simple warm-start procedure that initializes the ADMM variables v and λ . In particular, the initial values v^0 and λ^0 at sample time k are taken, respectively, as the optimal solutions v^* and λ^* obtained at sample time $k-1$, shifted $n+m+n_h$ positions forward. As this method does not determine the last $n+m+n_h$ components of v^0 and λ^0 , we simply copy these components from v^* and λ^* obtained at $k-1$, respectively.

6. Hardware-in-the-loop results

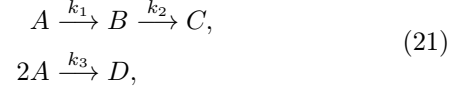
We set up a HiL scheme in which a Siemens S7-1500 PLC implements (11) and the estimator (7) to control the nonlinear system (1). The system dynamics are simulated via numerical integration on a PC, where the PLC solve times and communication delays affect the simulation. The PLC and the PC communicate via OPC UA ([Mahnke et al., 2009](#)), with the former acting as the OPC server and the latter as the client. The PLC operates in cyclic mode: this is an asynchronous mode of operation, where a new cycle begins immediately after the previous one ends, and its duration depends on the tasks executed within the cycle (e.g., ADMM iterations, monitoring or communication), see [Krupa et al. \(2021b\)](#). To avoid excessive consecutive CPU time on the solver task, we distribute the ADMM iterations across multiple PLC cycles, performing a fixed number of iterations in each cycle and verifying the termination criterion at the end. If satisfied, the control input is applied to the system; otherwise, the PLC continues to iterate from its last state. This approach allows other processes in each cycle to run more frequently rather than waiting for the optimization solver to finish. Further details on splitting the ADMM iterations on PLCs can be found in [Krupa et al. \(2021b\)](#).

We use the probabilistic validation approach from Section 4 to select the hyperparameters of the MPCT controller and to validate its long-term operation. Specifically, we select a set of back-off parameters to tighten the model constraints, and the weights β used for the soft constraints. Since we consider constraint satisfaction to be critical in this case, we aim to reduce constraint violations while keeping the number of iterations and computation time of the MPC solver low.

6.1. Testing system: continuous stirred-tank reactor

We consider a realistic model of a CSTR equipped with a cooling jacket, described in [Subramanian et al. \(2015\)](#). The main reaction, R_{AB} , is the transformation of a substance A into a product B . However, A also undergoes an undesirable parallel reaction, R_{AD} , producing a product D . Additionally, an unwanted consecutive reaction, R_{BC} ,

transforms B into a substance C . The whole process is summarized as



where $k_i, i \in \mathbb{I}_1^3$, are the respective reaction velocities. The system is described by the nonlinear differential equations

$$\dot{c}_A = \frac{F_I}{V_R} (c_{A0} - c_A) - k_1(\theta) c_A - k_3(\theta) c_A^2, \quad (22a)$$

$$\dot{c}_B = -\frac{F_I}{V_R} c_B + k_1(\theta) c_A - k_2(\theta) c_B, \quad (22b)$$

$$\dot{\theta} = \frac{F_I}{V_R} (\theta_d - \theta) - \frac{1}{\rho C_p} (k_1(\theta) c_A \Delta H_{R_{AB}} + k_2(\theta) c_B \Delta H_{R_{BC}} \\ + k_3(\theta) c_A^2 \Delta H_{R_{AD}}) + \frac{k_w A_R}{\rho C_p V_R} (\theta_K - \theta), \quad (22c)$$

$$\dot{\theta}_K = \frac{1}{m_K C_{pK}} (P_K + k_w A_R (\theta - \theta_K)), \quad (22d)$$

where c_A [mol/l] and c_B [mol/l] are the concentrations of A and B , respectively, and θ [°C] and θ_K [°C] are the temperatures of the reactor and cooling jacket, respectively. Each velocity k_i depends on the temperature θ as

$$k_i(\theta) = k_{i0} \cdot \exp\left(\frac{E_i}{\theta + 273.15}\right), \quad i \in \mathbb{I}_1^3. \quad (23)$$

The system has two inputs: the normalized input flow $F_N \doteq \frac{F_I}{V_R}$ [h⁻¹]; and the heat removal power P_K [kJ/h] of the cooling jacket. We consider two controlled outputs: the concentration c_B ; and the production rate of B , that is, $p_B \doteq c_B F_I$ [mol/h]. Table 1 includes a full list of the system parameters, with further details available in [Subramanian et al. \(2015\)](#). The constraints considered are $3 \leq F_N \leq 35$, $-9000 \leq P_K \leq 0$, $\theta \leq 117$, $c_B \geq 0.72$ and $p_B \geq 155$. Note that the constraint on p_B is a coupled state-input constraint. Additionally, the system is subject to disturbances due to fluctuations in the temperature θ_d of the input flow F_I , which we model according to the discrete-time Singer model

$$\theta_d(k+1) = 0.99 \cdot \theta_d(k) + (1 - 0.99) \cdot \theta_0 + w_d(k), \quad (24)$$

where $\theta_0 = 104.9$ °C is the nominal temperature value and $w_d(k)$ is a white Gaussian noise sampled from a normal distribution with zero mean and variance 0.01.

We apply a low-pass filter to the control inputs, defined by

$$\dot{u}_f(t) = T_f^{-1} (u(t) - u_f(t)), \quad (25)$$

where $T_f \doteq \text{diag}((T_{F_N}, T_{P_K}))$ are the filter time constants (see Table 1), $u_f \doteq (F_N, P_K) \in \mathbb{R}^m$ are the filtered inputs applied in (22), and $u \in \mathbb{R}^m$ the inputs of the filter, computed by the MPCT solver. Then, we extend the system dynamics by incorporating (25) into (22), resulting in a plant with state $x \doteq (c_A, c_B, \theta, \theta_K, u_f) \in \mathbb{R}^n$, input $u \in \mathbb{R}^m$, and output $y \doteq (c_B, p_B) \in \mathbb{R}^p$. The use of a

Parameter	Symbol	Value	Unit
Collision factor of R_{AB}	k_{10}	$1.287 \cdot 10^{12}$	[1/h]
Collision factor of R_{BC}	k_{20}	$1.287 \cdot 10^{12}$	[1/h]
Collision factor of R_{AD}	k_{30}	$9.043 \cdot 10^9$	[1/(mol·h)]
Activation energy of R_{AB}	E_1	-9758.3	[K]
Activation energy of R_{BC}	E_2	-9758.3	[K]
Activation energy of R_{AD}	E_3	-8560	[K]
Concentration of A in F_I	c_{A0}	5.1	[mol/l]
Temperature of fluid in F_I	θ_d	102–108	[°C]
Enthalpy of R_{AB}	$\Delta H_{R_{AB}}$	4.2	[kJ/mol]
Enthalpy of R_{BC}	$\Delta H_{R_{BC}}$	-11	[kJ/mol]
Enthalpy of R_{AD}	$\Delta H_{R_{AD}}$	-41.85	[kJ/mol]
Density of fluid in F_I	ρ	0.9342	[kg/l]
Heat capacity	C_p	3.01	[kJ/(kg·K)]
Heat transfer coefficient for cooling jacket	k_w	4.032	[kJ/(hm ² ·K)]
Surface of cooling jacket	A_R	0.215	[m ²]
Reactor volume	V_R	0.01	[m ³]
Coolant mass	m_K	5	[kg]
Heat capacity of coolant	C_{pK}	2	[kJ/(kg·K)]
Filter time constant of F_N	T_{F_N}	250	[s]
Filter time constant of P_K	T_{P_K}	125	[s]

Table 1: Parameters of the CSTR system.

low-pass input filter is common in real industrial scenarios to avoid sudden changes in the inputs, improving the life expectancy of the actuators. Indeed, most industrial valves integrate a local PID controller for this reason.

A discrete linear model (3) of the system is obtained by linearizing around the equilibrium point

$$F_N = 25 \text{ h}^{-1}, P_K = -4000 \text{ kJ/h}, c_A = 3.161 \text{ mol/l}, \quad (26)$$

$$c_B = 0.912 \text{ mol/l}, \theta = 108.53^\circ\text{C}, \theta_K = 103.91^\circ\text{C},$$

and discretizing with a sample time of 75 seconds. Finally, we take the matrices in (4c) as $E = C$ and $F = 0$.

6.2. Controller and estimator parameters

For the practical MPCT formulation (11), we select a prediction horizon length $N = 7$, and the weight matrices as $Q = \text{diag}((0.1, 0.1, 5, 5, 20, 30))$, $R = \text{diag}((20, 30))$, $S = \text{diag}((10, 50))$ and $T = \text{diag}((0.7, 0.7, 35, 35, 10, 50))$. For ADMM, we take: $\rho = 40$, $\epsilon_p = 5 \cdot 10^{-3}$, $\epsilon_d = 1 \cdot 10^{-3}$. For better performance of ADMM, we precondition the MPC optimization problem by scaling the state and input using the matrices $N_x = \text{diag}((5, 20, 1, 1, 2, 10^{-3}))$ and $N_u = \text{diag}((2, 10^{-3}))$, respectively, and the coupled constraints (4c) using $N_c = \text{diag}((20, 0.5))$. For further details on this procedure, see Krupa et al. (2021b).

As explained in Maeder et al. (2009), the only requirement for the design of L_x and L_d is that the resulting estimator (7) is stable. In our case, we exploit the controller-observer duality by applying the LQR design method to (7), with weights for the LQR stage cost $R' = \text{diag}((10^3, 10^3))$ and $Q' = \text{diag}((1, 0.01, 1, 1, 10, 10, 10^4, 10^4))$. Furthermore, as the resulting linear model has no integrator states, we take $B_d = 0$ to simplify the observer; see Maeder et al.

(2009) for further details and guidelines on the design of the estimator for offset-free control.

In the next subsection, we discuss the choice of the soft constraints weights β and the back-off parameters of the controller through the probabilistic validation procedure detailed in Section 4.

6.3. Validation experiments design

The selection of hyperparameters in MPC controllers, such as the cost function matrices, is typically made offline through simulations. However, the impact that some hyperparameters will have on the controller, such as the weights β and back-off parameters, can be more difficult to estimate. Therefore, we fix some parameters in advance, and explore multiple controller configurations depending on the remaining, harder-to-tune parameters.

We are interested in validating the long-term behavior of the closed-loop system for a given selection of MPCT hyperparameters. Specifically, we aim to verify that the controller performs satisfactorily under the real operating conditions of the plant, where its outputs are required to track a piecewise constant reference. To this end, each of the N_s validation experiments consists of a closed-loop simulation of the system trajectory over $N_t = 100$ sample times, where:

- Before recording each experiment, the closed-loop system is subject to an initialization phase that lasts 40 sample times using a random reference $y_{r1} \doteq (c_{Br_1}, p_{Br_1})$, with components c_{Br_1} and p_{Br_1} sampled from uniform distributions within the intervals $[0.73, 1.094]$ and $[155, 301]$, respectively. Here, the state x starts at the equilibrium point (26), the Singer model (24) at θ_0 , and the estimator (7) at the origin. Therefore, the time index $k = 0$ denotes the first sample time following the initialization phase, where the closed-loop system is already in steady-state regime.
- At a random time instant t_r sampled from a uniform distribution of integers in the range $[10, 50]$, the reference changes to a new value $y_{r2} \doteq (c_{Br_2}, p_{Br_2})$, sampled from the same probability distribution as y_{r1} .

The length of the experiments and the time window for changing the reference were selected so that the experiments could capture both the transient and the steady-state behavior of the closed-loop system. We note that the controller design in Section 6.2 typically steers the system to steady-state regime in approximately 40 sample times, which explains the selected length of the initialization phase. Note also that the reference is modeled as a random variable to validate the controller in a wide range of operating regimes.

Referring to the nomenclature used in Section 4, in our experimental setup, a sample w drawn from \mathcal{W} includes: the random reference values y_{r1} and y_{r2} ; the reference change time instant t_r ; the initial state $x(0)$; the

estimate of the initial state $\hat{x}(0)$ and disturbance $\hat{d}(0)$; the sequence of disturbances $\theta_d(0), \dots, \theta_d(N_t - 1)$; and any other stochastic variable affecting the closed-loop system, e.g., the communication times along an experiment.

Remark 4. *The proposed validation experiments are taken to resemble the typical operation of the plant, capturing both the transient and steady-state behavior of the closed-loop system. That is, they are structured so that the probabilistic bounds obtained are meaningful for assessing long-term closed-loop performance, either under a constant reference or when it undergoes a step change.*

6.4. Performance indicators and hyperparameters

We consider the performance indicators

$$\begin{aligned}\phi^1(w) &\doteq \sum_{k=0}^{N_t-1} \rho_\theta (\max(\theta(k) - \bar{\theta}, 0))^2 \\ &\quad + \rho_c (\max(\underline{c}_B - c_B(k), 0))^2 \\ &\quad + \rho_p (\max(\underline{p}_B - p_B(k), 0))^2, \end{aligned}\quad (27a)$$

$$\phi^2(w) \doteq \max_{k=0, \dots, N_t-1} N_{\text{iter}}(k), \quad (27b)$$

where $\bar{\theta} = 117$, $\underline{c}_B = 0.72$ and $\underline{p}_B = 155$ are the bounds of the constrained variables as defined in Section 6.1. The positive scalars ρ_θ , ρ_c and ρ_p normalize and weight the violation of the constraints, and $N_{\text{iter}}(k)$ denotes the number of iterations performed by the ADMM algorithm at sample time k . We select $\rho_\theta = 30$, $\rho_c = 150$ and $\rho_p = 1$.

The performance indicator ϕ^1 defined in (27a) gives a measure of constraint violations during a closed-loop experiment. We do not penalize constraint violations of the inputs, as the applied inputs are hard constrained by (11f) and fit the form required in Section 6.1. The $\max(\cdot)$ terms in ϕ^1 are squared to strongly penalize cases in which the variables significantly exceed their bounds. Note that $\phi^1(\cdot) = 0$ if and only if the closed-loop trajectories are feasible throughout the entire simulation. The indicator ϕ^2 in (27b) returns the maximum number of ADMM iterations throughout an experiment. As the number of ADMM iterations is directly related to the computation time of the solver, we use ϕ^2 to validate that the control action $u(k)$ is computed in a time that is significantly shorter than the sample time of the system.

Through probabilistic validation, we propose selecting one among M different controllers, determined by all possible combinations of the hyperparameter values

$$\begin{aligned}\bar{\eta}_\theta &\in \{0, 1.5, 3\}, \quad \underline{\eta}_c \in \{0, 0.04, 0.08\}, \\ \underline{\eta}_p &\in \{0, 10, 20\}, \quad \beta \in \{\mathbf{1}_{n_\theta} \cdot 100, \mathbf{1}_{n_\theta} \cdot 300\},\end{aligned}$$

where $\bar{\eta}_\theta$, $\underline{\eta}_c$ and $\underline{\eta}_p$ tighten the bounds $\bar{\theta}$, \underline{c}_B and \underline{p}_B , respectively. This results in a total of $M = 54$ candidate controllers. As in this particular case we only consider

vectors with identical elements for β , given a scalar $c \in \mathbb{R}$, we write $\beta = c$ to denote $\beta = \mathbf{1}_{n_\theta} \cdot c$ in what follows.

Setting $\delta = 1 \cdot 10^{-6}$, $\epsilon = 0.03$ and $r = 5$, and applying (14) with $K = 2$, we find that performing $N_s \geq 1156$ closed-loop experiments is sufficient to individually bound the probabilities defined in (12) with a confidence of at least $1 - \delta$. Accordingly, we select $N_s = 1156$.

6.5. Validation experiments

We note that Proposition 1 does not require evaluating all the M candidate controllers for (12) to hold individually for each controller. In other words, (12) is valid for the controller setup i , as soon as $\phi_i^{\ell, [r]}$ is experimentally evaluated. Therefore, once an acceptable controller is found, the performance of other candidate setups does not need to be assessed (Karg et al., 2021).

The left part of Table 2 shows the performance of the r -th worst case, as measured by the indicators in (27), obtained for a subset of the M controllers. Column “feasible trajectories” displays the percentage of experiments (out of N_s) that resulted in no constraint violations. The results indicate that, as the back-off parameters $\bar{\eta}_\theta$, $\underline{\eta}_c$ and $\underline{\eta}_p$ increase, the number of experiments resulting in feasible trajectories grows. However, increasing β does not appear to significantly improve constraint satisfaction, while the number of ADMM iterations is negatively affected. Another point to consider is that, even though controllers with larger back-off may seem to perform better according to Table 2, excessive back-offs can often make the reference $(x_r(k), u_r(k))$ provided by (8) not admissible, and make the controller behave too conservatively. Since constraint satisfaction is considered to be crucial in this case study, we select a set of back-off parameters that, without being too large, provides low levels of constraint violations. Specifically, we select the controller with parameters $\{\bar{\eta}_\theta, \underline{\eta}_c, \underline{\eta}_p, \beta\} = \{1.5, 0.08, 20, 100\}$, which we denote as C_1 . For comparison, we denote by C_0 the controller with $\beta = 100$ and no back-off, i.e., $\{\bar{\eta}_\theta, \underline{\eta}_c, \underline{\eta}_p, \beta\} = \{0, 0, 0, 100\}$. We conclude from Table 2 that in a new experiment, with high confidence $1 - \delta$, the closed-loop system will violate the constraints by no more than 0.0045, as measured by ϕ^1 defined in (27a), with a probability of at least $100 \cdot (1 - \epsilon) = 97\%$. With the same confidence and probability bound, the maximum number of ADMM iterations in a new experiment will be at most 246. Figure 1 shows the closed-loop experiment resulting in the 5-th worst-case performance according to ϕ^1 .

To empirically validate the probabilistic bounds obtained, each controller was tested in 1000 new i.i.d. closed-loop experiments. The right part of Table 2 shows the results, which confirm the probabilistic bounds and indicate that the number of experiments in which the controllers exceed their thresholds is rather small. We note that respecting the probabilistic bounds for both performance indicators ϕ^1 and ϕ^2 simultaneously is very frequent.

Hyper-parameters $\{\bar{\eta}_\theta, \underline{\eta}_c, \underline{\eta}_p, \beta\}$	Controller validation			Empirical verification of (12)		
	Constraint violations $\phi^{1,[5]}$	ADMM iterations $\phi^{2,[5]}$	Feasible trajectories ($\phi^1 = 0$)	Experiments where $\phi^1 \leq \phi^{1,[5]}$	Experiments where $\phi^2 \leq \phi^{2,[5]}$	Feasible trajectories ($\phi^1 = 0$)
$\{0, 0, 0, 100\}$	6.6753	177	96.9%	99.6%	99.2%	96.3%
$\{0, 0, 0, 300\}$	6.6016	637	96.9%	99.6%	99.7%	96.3%
$\{0, 0, 10, 100\}$	1.4256	240	98.1%	99.5%	99.1%	97.6%
$\{0, 0, 10, 300\}$	1.4414	736	98.1%	99.5%	99.7%	97.6%
$\{1.5, 0.08, 20, 100\}$	0.0045	246	99.5%	99.7%	99.5%	99.6%
$\{1.5, 0.08, 20, 300\}$	0.0048	740	99.5%	99.7%	99.5%	99.6%
$\{3, 0.08, 20, 100\}$	0	246	99.8%	99.9%	99.2%	99.9%
$\{3, 0.08, 20, 300\}$	0	740	99.8%	99.9%	99.5%	99.9%

Table 2: On the left: Probabilistic bounds (see (12)) obtained for a subset of the $M = 54$ candidate controllers with $K = 2$, $\delta = 1 \cdot 10^{-6}$, $r = 5$, $\epsilon = 0.03$ and $N_s = 1156$ according to (14). The selected controller C_1 is highlighted in bold. On the right: Empirical verification of the probabilistic bounds. The percentage of feasible trajectories is to be considered as complementary information (not covered in this case by the result of Proposition 1).

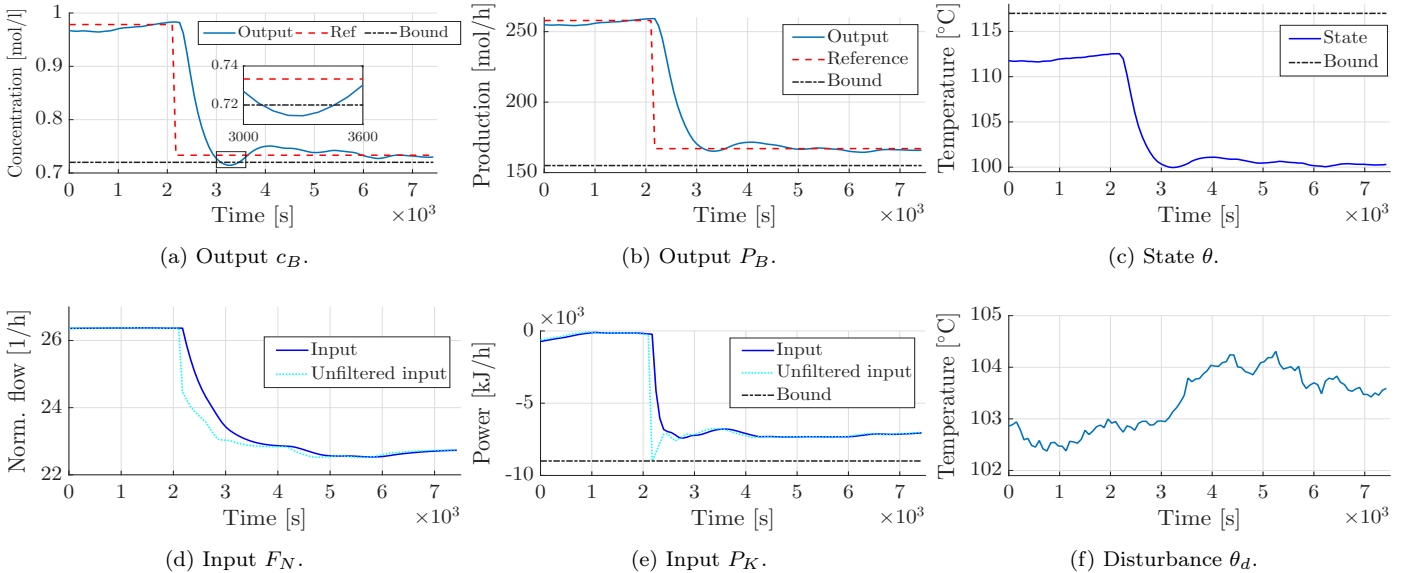


Figure 1: Closed-loop simulation of the CSTR controlled with C_1 . This experiment corresponds to the 5-th worst case of C_1 , where $\phi^1(\cdot) = 0.0045$ (see Table 2).

To illustrate that constraint tightening can exacerbate the issue of generating infeasible references $(x_r(k), u_r(k))$ in (8), thus preventing the system from achieving offset-free tracking to constant output references y_r , Figure 2 compares the controllers C_1 and C_0 in one of the N_s PLC validation experiments. The results show that, in this particular case, offset-free tracking of the output c_B is not achieved with the selected controller C_1 , whereas the controller C_0 does achieve offset-free tracking (albeit at the expense of constraint violations).

To assess reference tracking performance of the controller C_1 along the N_s experiments, we compute, for each experiment $j \in \mathbb{I}_1^{N_s}$, the distance between each output and the reference value y_{r2} between the time instant t_r in which the reference changes, and $t_r + 50$. In addition, we repeat the process for C_0 to illustrate how back-off affects the abil-

ity of the controller to reach the output reference. The results are shown in Figure 3. Comparing Figure 3a with 3b, and 3c with 3d, we observe that the tracking performance improves when using C_0 compared to C_1 (see the zoomed-in parts), as with the former, offset is reduced in general and a notably larger number of experiments achieve offset-free tracking, of course at the expense of higher constraint violations. However, many experiments still cannot reach the reference with C_0 , partly because a significant number of experiments consider output references y_{r2} that are not admissible due to the real system constraints. Indeed, this situation is not unusual in practice, where the operator may not know if the selected reference is admissible, but still aims to stabilize the system as close as possible to it.

To better assess the effect of back-off and the actual tracking performance of the controllers, we compute the

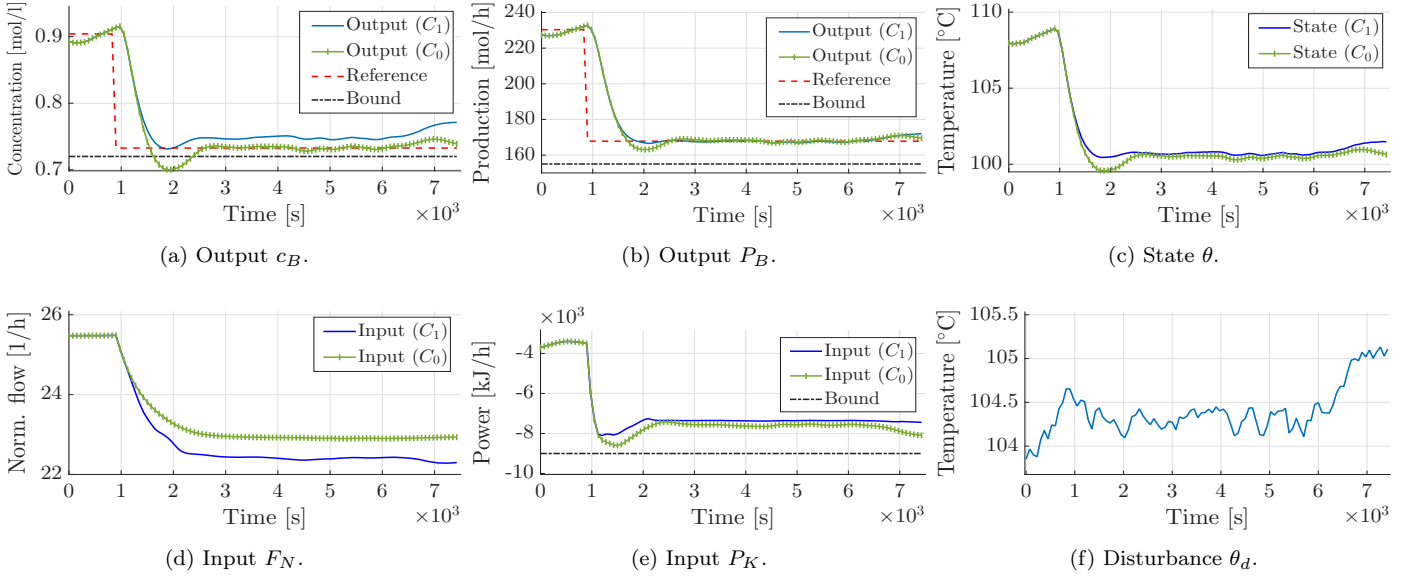


Figure 2: Comparison of closed-loop simulations of the CSTR system using the controllers C_1 and C_0 . A case with nonadmissible reference pairs $(x_r(k), u_r(k))$ due to back-off.

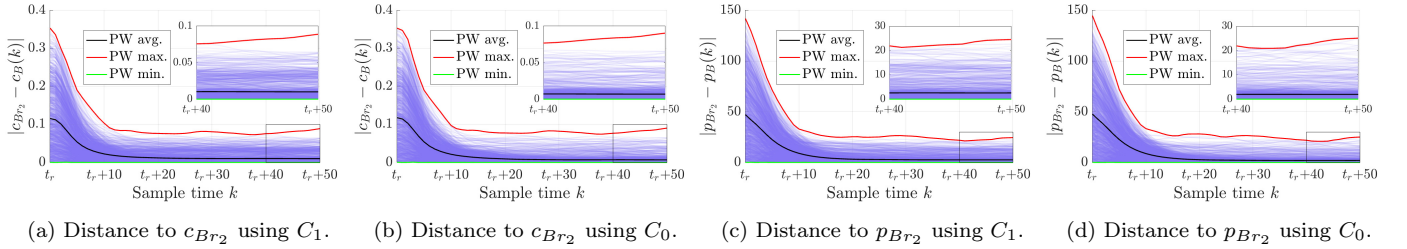


Figure 3: Comparison of distances from outputs to reference y_r using controllers C_1 and C_0 . In the legend, ‘‘PW’’ stands for ‘‘point-wise’’.

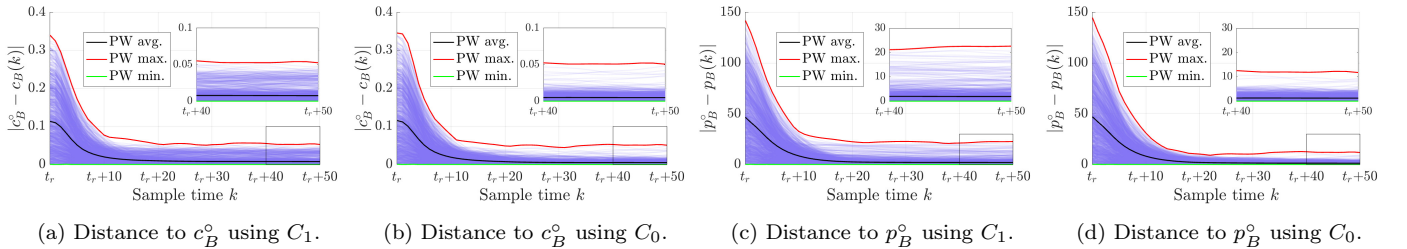
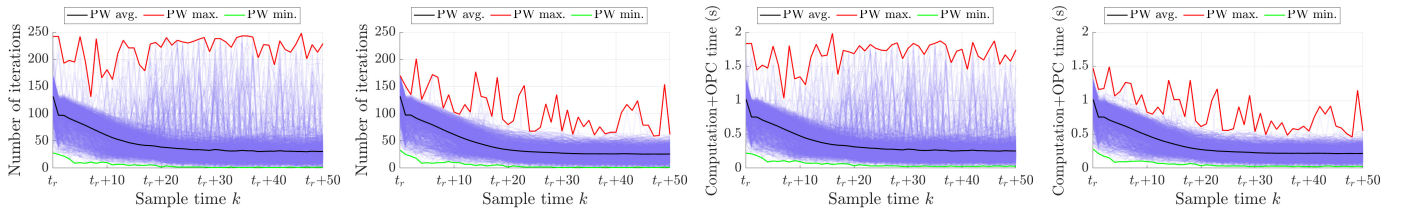


Figure 4: Comparison of distances from the outputs to the admissible reference y^o using controllers C_1 and C_0 .

distance to the admissible steady output $y^o \doteq (C_B^o, p_B^o)$. This output is obtained in two steps: (i) given y_{r2} , compute the steady state-input pair (x_u, u_u) to which the closed-loop system (with $\theta_d = \theta_0$) would converge in the absence of constraints; and (ii) considering the system constraints (2), determine the admissible steady output y^o corresponding to the steady state-input (x_c, u_c) obtained by minimizing the distance between u_c and u_u . The results are illustrated in Figure 4, where we observe that, although back-off helps enforce the constraints, in many cases it prevents the system from approaching y^o , in contrast to most cases without back-off.

Figure 5 shows a comparison between the controllers C_1 and C_0 in terms of number of iterations and computation-plus-communication time obtained for the N_s experiments between the time instants t_r and $t_r + 50$. Note that, although the controller C_0 provides in general a lower number of iterations and times due to a reduced occurrence of active constraints, the controller C_1 provides rather acceptable results while ensuring small constraints violations, yielding a maximum time on the PLC of 1.98 seconds, which is considerably shorter than the sample time of 75 seconds.

In terms of memory efficiency, the implementation of



(a) Number of iterations using C_1 . (b) Number of iterations using C_0 . (c) Input availability time using C_1 . (d) Input availability time using C_0 .

Figure 5: Comparison of number of iterations and time required to obtain the input using controllers C_1 and C_0 .

the estimator (7), the solver for (11) and the reference calculator (8) required 0.73 MB of memory in the PLC, which constitutes only a 3% of the 24 MB available.

7. Conclusions

This article has demonstrated the viability of controlling a real (nonlinear) system using a refined linear MPC controller implemented on industrial embedded hardware. Combined with an offset-free scheme, it proved to be a practical solution thanks to several key features: an artificial reference that avoids the need to provide an admissible reference; soft constraints that ensure feasibility of the MPC optimization problem; and back-off parameters to adjust the model constraints to satisfy the actual system constraints. In addition, we proposed a probabilistic framework that enables the selection of critical controller parameters and the validation of the long-term closed-loop system operation. By means of a structure-exploiting solver, we showed how the formulation can be implemented efficiently, according to embedded systems capabilities. For the numerical experiments, the formulation was implemented on a Siemens S7-1500 PLC to control a nonlinear CSTR system in a HiL setup. The results confirmed the effectiveness of both the formulation and the probabilistic framework, obtaining a controller with probabilistic bounds on critical aspects such as constraint violations and computational efficiency, thereby meeting the requirements of real-world operation. Overall, this work contributes to bridging the gap between academic research and industrial practice.

Declaration of competing interest

The authors declare that they have no known competing financial interests or personal relationships that could have appeared to influence the work reported in this paper.

Acknowledgments

This work was supported from grants PID2022-142946NA-I00 and PID2022-141159OB-I00, funded by MICIU/AEI/10.13039/501100011033 and by ERDF/EU.

V. Gracia acknowledges support from grant PREP2022-000136 funded by MICIU/AEI/ 10.13039/501100011033 and by ESF+.

F. Fele also gratefully acknowledges support from grant RYC2021-033960-I funded by MICIU/AEI/ 10.13039/501100011033 and European Union NextGenerationEU/PRTR.

References

Abuin, P., Ferramosca, A., Toffanin, C., Magni, L., Gonzalez, A.H., 2022. Artificial pancreas under periodic MPC for trajectory tracking: handling circadian variability of insulin sensitivity. IFAC-PapersOnLine 55, 196–201. doi:[10.1016/j.ifacol.2022.09.023](https://doi.org/10.1016/j.ifacol.2022.09.023).

Alphonsus, E.R., Abdullah, M.O., 2016. A review on the applications of programmable logic controllers (PLCs). Renewable and Sustainable Energy Reviews 60, 1185–1205. doi:[10.1016/j.rser.2016.01.025](https://doi.org/10.1016/j.rser.2016.01.025).

Beck, A., 2017. First-Order Methods in Optimization. MOS-SIAM Series on Optimization, SIAM – Society for Industrial and Applied Mathematics. doi:[10.1137/1.9781611974997](https://doi.org/10.1137/1.9781611974997).

Boyd, S., 2009. Convex Optimization. 7 ed., Cambridge University Press. doi:[10.1017/CBO9780511804441](https://doi.org/10.1017/CBO9780511804441).

Boyd, S., Parikh, N., Chu, E., Peleato, B., Eckstein, J., 2011. Distributed optimization and statistical learning via the alternating direction method of multipliers. Foundations and Trends® in Machine Learning 3, 1–122. doi:[10.1561/2200000016](https://doi.org/10.1561/2200000016).

Camacho, E.F., Alba, C.B., 2007. Model Predictive Control. 2 ed., Springer London. doi:[10.1007/978-0-85729-398-5](https://doi.org/10.1007/978-0-85729-398-5).

Ferreau, H., Almér, S., Verschueren, R., Diehl, M., Frick, D., Domahidi, A., Jerez, J., Stathopoulos, G., Jones, C., 2017. Embedded optimization methods for industrial automatic control. IFAC-PapersOnLine 50, 13194–13209. doi:[10.1016/j.ifacol.2017.08.1946](https://doi.org/10.1016/j.ifacol.2017.08.1946).

Fletcher, R., 2000. Practical Methods of Optimization. John Wiley & Sons, Ltd. doi:[10.1002/9781118723203](https://doi.org/10.1002/9781118723203).

Frison, G., Diehl, M., 2020. HPIPM: A high-performance quadratic programming framework for model predictive control. IFAC-PapersOnLine 53, 6563–6569. doi:[10.1016/j.ifacol.2020.12.073](https://doi.org/10.1016/j.ifacol.2020.12.073).

Gracia, V., Krupa, P., Limon, D., Alamo, T., 2024a. Efficient implementation of MPC for tracking using

ADMM by decoupling its semi-banded structure, in: 2024 European Control Conference (ECC), pp. 2718–2723. doi:[10.23919/ECC64448.2024.10591273](https://doi.org/10.23919/ECC64448.2024.10591273).

Gracia, V., Krupa, P., Limon, D., Alamo, T., 2024b. Implementation of soft-constrained MPC for tracking using its semi-banded problem structure. *IEEE Control Systems Letters* 8, 1499–1504. doi:[10.1109/LCSYS.2024.3407609](https://doi.org/10.1109/LCSYS.2024.3407609).

He, B., Yuan, X., 2012. On the $O(1/n)$ convergence rate of the Douglas–Rachford alternating direction method. *SIAM Journal on Numerical Analysis* 50, 700–709. doi:[10.1137/110836936](https://doi.org/10.1137/110836936).

Jerez, J.L., Goulart, P.J., Richter, S., Constantinides, G.A., Kerrigan, E.C., Morari, M., 2014. Embedded online optimization for model predictive control at mega-hertz rates. *IEEE Transactions on Automatic Control* 59, 3238–3251. doi:[10.1109/TAC.2014.2351991](https://doi.org/10.1109/TAC.2014.2351991).

Karg, B., Alamo, T., Lucia, S., 2021. Probabilistic performance validation of deep learning-based robust NMPC controllers. *International Journal of Robust and Non-linear Control* 31, 8855–8876. doi:[10.1002/rnc.5696](https://doi.org/10.1002/rnc.5696).

Kerrigan, E.C., Maciejowski, J.M., 2000. Soft constraints and exact penalty functions in model predictive control, in: Control 2000 Conference, Cambridge, pp. 2319–2327. <http://hdl.handle.net/10044/1/10241>.

Krupa, P., Camara, J., Alvarado, I., Limon, D., Alamo, T., 2021a. Real-time implementation of MPC for tracking in embedded systems: Application to a two-wheeled inverted pendulum, in: 2021 European Control Conference (ECC), pp. 669–674. doi:[10.23919/ECC54610.2021.9654899](https://doi.org/10.23919/ECC54610.2021.9654899).

Krupa, P., Gracia, V., Limon, D., Alamo, T., 2020. SPCIES: Suite of predictive controllers for industrial embedded systems. <https://github.com/GepocUS/Spies>.

Krupa, P., Köhler, J., Ferramosca, A., Alvarado, I., Zeilinger, M.N., Alamo, T., Limon, D., 2024. Model predictive control for tracking using artificial references: Fundamentals, recent results and practical implementation, in: 2024 IEEE 63rd Conference on Decision and Control (CDC), pp. 2977–2991. doi:[10.1109/CDC56724.2024.10886854](https://doi.org/10.1109/CDC56724.2024.10886854).

Krupa, P., Limon, D., Alamo, T., 2021b. Implementation of model predictive control in programmable logic controllers. *IEEE Transactions on Control Systems Technology* 29, 1117–1130. doi:[10.1109/TCST.2020.2992959](https://doi.org/10.1109/TCST.2020.2992959).

Limon, D., Alvarado, I., Alamo, T., Camacho, E., 2008. MPC for tracking piecewise constant references for constrained linear systems. *Automatica* 44, 2382–2387. doi:[10.1016/j.automatica.2008.01.023](https://doi.org/10.1016/j.automatica.2008.01.023).

Lowenstein, K.F., Bernardini, D., Patrinos, P., 2024. QPALM-OCP: A Newton-type proximal augmented lagrangian solver tailored for quadratic programs arising in model predictive control. *IEEE Control Systems Letters* 8, 1349–1354. doi:[10.1109/LCSYS.2024.3410638](https://doi.org/10.1109/LCSYS.2024.3410638).

Maeder, U., Borrelli, F., Morari, M., 2009. Linear offset-free model predictive control. *Automatica* 45, 2214–2222. doi:[10.1016/j.automatica.2009.06.005](https://doi.org/10.1016/j.automatica.2009.06.005).

Mahnke, W., Leitner, S.H., Damm, M., 2009. OPC Unified Architecture. Springer-Verlag Berlin Heidelberg. doi:[10.1007/978-3-540-68899-0](https://doi.org/10.1007/978-3-540-68899-0).

Mammarella, M., Alamo, T., Lucia, S., Dabbene, F., 2020. A probabilistic validation approach for penalty function design in stochastic model predictive control. *IFAC-PapersOnLine* 53, 11271–11276. doi:[10.1016/j.ifacol.2020.12.362](https://doi.org/10.1016/j.ifacol.2020.12.362).

Moscato, S., Sanalitro, D., Stella, G., Bucolo, M., 2024. Model predictive control framework for slug flow microfluidics processes. *Control Engineering Practice* 148, 105944. doi:[10.1016/j.conengprac.2024.105944](https://doi.org/10.1016/j.conengprac.2024.105944).

Nubert, J., Köhler, J., Berenz, V., Allgöwer, F., Trimpe, S., 2020. Safe and fast tracking on a robot manipulator: Robust MPC and neural network control. *IEEE Robotics and Automation Letters* 5, 3050–3057. doi:[10.1109/LRA.2020.2975727](https://doi.org/10.1109/LRA.2020.2975727).

O'Donoghue, B., 2021. Operator splitting for a homogeneous embedding of the linear complementarity problem. *SIAM Journal on Optimization* 31, 1999–2023. doi:[10.1137/20M1366307](https://doi.org/10.1137/20M1366307).

Rawlings, J.B., Mayne, D.Q., Diehl, M., 2017. Model Predictive Control: Theory, Computation, and Design. 2 ed., Nob Hill Publishing. <https://sites.engineering.ucsb.edu/~jbraw/mpc>.

Santos, T.L., Bonzanini, A.D., Heirung, T.A.N., Mesbah, A., 2019. A constraint-tightening approach to nonlinear model predictive control with chance constraints for stochastic systems, in: 2019 American Control Conference (ACC), pp. 1641–1647. doi:[10.23919/ACC.2019.8814623](https://doi.org/10.23919/ACC.2019.8814623).

Stellato, B., Banjac, G., Goulart, P., Bemporad, A., Boyd, S., 2020. OSQP: An operator splitting solver for quadratic programs. *Mathematical Programming Computation* 12, 637–672. doi:[10.1007/s12532-020-00179-2](https://doi.org/10.1007/s12532-020-00179-2).

Subramanian, S., Lucia, S., Engel, S., 2015. Adaptive multi-stage output feedback NMPC using the extended Kalman filter for time varying uncertainties applied to a cstr. *IFAC-PapersOnLine* 48, 242–247. doi:[10.1016/j.ifacol.2015.11.290](https://doi.org/10.1016/j.ifacol.2015.11.290).

Tylavsky, D., Sohie, G., 1986. Generalization of the matrix inversion lemma. *Proceedings of the IEEE* 74, 1050–1052. doi:[10.1109/PROC.1986.13587](https://doi.org/10.1109/PROC.1986.13587).

Valencia-Palomo, G., Rossiter, J., 2011. Efficient suboptimal parametric solutions to predictive control for PLC applications. *Control Engineering Practice* 19, 732–743. doi:[10.1016/j.conengprac.2011.04.001](https://doi.org/10.1016/j.conengprac.2011.04.001).

Wabersich, K.P., Krishnadas, R., Zeilinger, M.N., 2022. A soft constrained MPC formulation enabling learning from trajectories with constraint violations. *IEEE Control Systems Letters* 6, 980 – 985. doi:[10.1109/LCSYS.2021.3087968](https://doi.org/10.1109/LCSYS.2021.3087968).